

## Extending the Simultaneous Heat and Water (SHAW) Model to Simulate Carbon Dioxide and Water Fluxes over Wheat Canopy

Qiang Yu

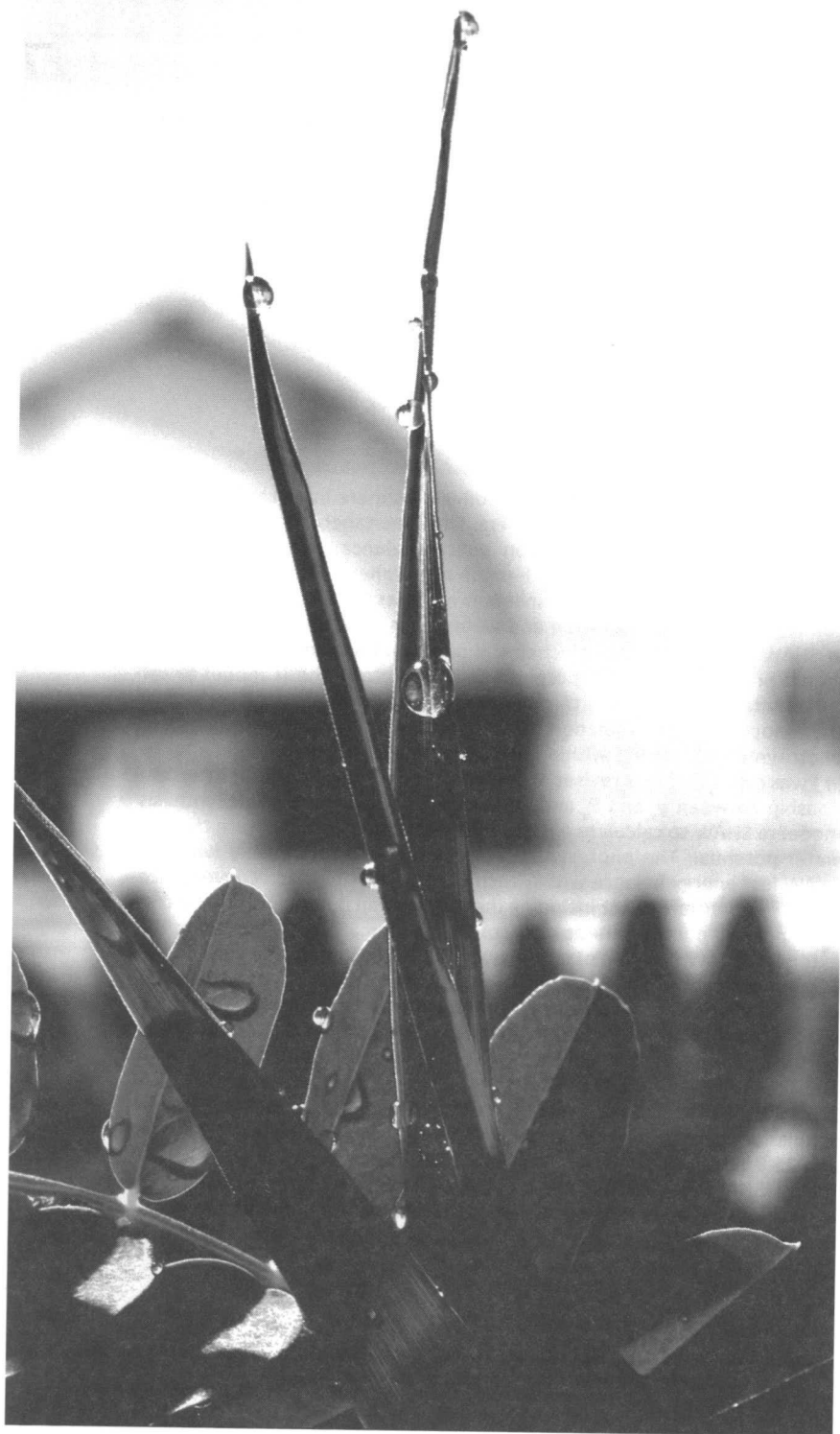
Institute of Geographical Sciences and Natural Resources Research, Chinese Academy of Sciences, Beijing

Gerald N. Flerchinger

USDA-ARS, Northwest Watershed Research Center, Boise, Idaho

### Abstract

Energy, water, and  $\text{CO}_2$  fluxes at the soil-atmosphere interface are of key interest among ecosystem researchers. The Simultaneous Heat and Water (SHAW) Model describes radiation energy balance, heat transfer, and water movement within the soil-plant-atmosphere continuum but has no plant growth or carbon assimilation modules. This study coupled the components of solar radiation and water transfer within a plant canopy in SHAW with a leaf-level biochemical photosynthesis model. The SHAW model provides leaf water potential to the photosynthesis model to calculate intercellular  $\text{CO}_2$  ( $C_i$ ) through stomatal control in each layer within the canopy, and solar radiation, air temperature and humidity to calculate photosynthetic rate ( $P_n$ ) within each canopy layer. Stomatal conductance ( $g_s$ ) was calculated by a revised Ball-Berry model, which describes the relationship between  $g_s$  and  $P_n$  and was a feedback from the photosynthesis model to SHAW to calculate energy and water transfer and in turn the leaf water potential. The photosynthesis model was run iteratively with the SHAW leaf energy balance within each canopy layer to reach convergence in leaf temperature. After including the relationship between stomatal conductance and photosynthetic rate, computed stomatal conductance in the extended SHAW (SHAW-Pn) model was able to respond to the variation of  $\text{CO}_2$  concentration. Validation of the photosynthesis model showed adequate simulations of responses of photosynthesis, transpiration, stomatal conductance, and  $C_i$  at leaf level to changes in light and  $\text{CO}_2$ . The SHAW-Pn performed excellently in simulating net radiation, sensible and latent heat, and  $\text{CO}_2$  fluxes over a winter wheat field in the North China Plain ( $36^\circ 57' \text{N}$ ,  $116^\circ 36' \text{E}$ , 28 m above sea level). The root mean square error (RMSE) of the simulation for net radiation, latent, and sensible heat fluxes was 36.1, 31.0, and 25.8  $\text{W m}^{-2}$ , respectively. The RMSE of  $\text{CO}_2$  flux simulation was 0.18  $\text{mg m}^{-2} \text{s}^{-1}$ . SHAW-Pn describes the biophysico-chemical processes and water and carbon cycles in the ecosystem, which can be a framework of vegetation response to atmospheric  $\text{CO}_2$  changes but needs incorporation of a detailed plant growth module.



USDA-NRCS, Rich Sanders

Energy balance at the soil–plant–atmosphere interface is an essential component in process-based ecological models (Cowan, 1965; Jarvis and McNaughton, 1986; Choudhury and Monteith, 1988; Chen and Coughenour, 1994; Williams et al., 1996; Wang and Leuning, 1998; Lakshmi and Wood, 1998; Calvet, 2000; Arora, 2003). The Simultaneous Heat and Water (SHAW) Model is a detailed energy balance model capable of simulating soil water, heat transfer, and evapotranspiration within a vertical, one-dimensional profile extending from the vegetation canopy, snow, residue cover, and soil surface to a specified depth within the soil (Flerchinger and Saxton, 1989; Flerchinger and Hanson, 1989; Flerchinger and Pierson, 1991; Flerchinger et al., 1994, 1996a, 1996b, 1998, 2003; Xiao et al., 2006). SHAW has been used for predicting these processes as well as soil freezing, snow melt, and related land surface processes. SHAW simulates water flow through a multispecies plant canopy along the soil–plant–atmosphere continuum and therefore can be extended to simulate CO<sub>2</sub> flux between atmosphere and vegetation after including the component of CO<sub>2</sub> assimilation by photosynthesis. This is a key factor in determining primary productivity, an important element in ecosystem modeling.

Photosynthesis and transpiration are closely related (Chaves, 1991). Simultaneous simulations of photosynthesis, stomatal processes, and gas diffusion processes can lead to better simulation of photosynthesis responses to environment (Collatz et al., 1991; McMurtrie et al., 1992; Leuning, 1995; Leuning et al., 1995; Yu and Wang, 1998; Yu et al., 2001; Tuzet et al., 2003). The stomatal model in SHAW, which is a function of leaf water potential only, will be improved by incorporating interactions between photosynthesis, transpiration, and stomatal conductance. The objectives of this paper were to (i) link a photosynthesis model with the SHAW model to simulate CO<sub>2</sub> fluxes in addition to water and energy fluxes and (ii) test the extended model against experimental data under a winter wheat (*Triticum aestivum* L.) cropping system in China. This coupling of SHAW with the photosynthesis model is referred to as SHAW-Pn.

## Model Descriptions

### The SHAW Model

SHAW was originally developed to model soil heat and water transfer at the land surface by Flerchinger and Saxton (1989) and modified by Flerchinger and Piereson (1991) to include transpiring plants and a plant canopy of mixed plant types. Flerchinger (2000) provides details of the current version of SHAW. A layered system is established to compute the heat and water fluxes through the plant canopy, snow, residue, and soil, and each layer is represented by an individual node. The plant canopy can be divided into as many as 10 layers. The leaf-area increment of each layer of wheat canopy was  $0.5 \text{ m}^2 \text{ m}^{-2}$  in this study. Computed surface energy balance fluxes include absorbed solar radiation, long-wave radiation exchange, and turbulent transfer of heat and vapor. Net radiation is determined by computing solar and long-wave radiation exchange between canopy layers, residue layers, and the soil surface. Sensible and latent heat fluxes of the surface energy balance are computed from temperature and vapor gradients between the canopy surface and the atmosphere by means of a bulk aerodynamic approach with stability corrections. Gradient-driven heat and vapor transfer within the canopy is determined by computing transfer between layers of the canopy and considering the source terms for heat and transpiration from the leaves for each layer within the canopy. The leaf energy balance is computed iteratively with heat and water vapor transfer equations and transpiration within the canopy. The wind speed profile within the canopy is assumed to decrease exponentially with leaf area.

Water flow within the plant is calculated assuming continuity in water potential throughout the plants and is controlled mainly by changes in stomatal resistance (Fig. 7-1, Eq. [1]).

$$T_j = \sum_{k=1}^{NS} \frac{\psi_k - \psi_{x,j}}{r_{r,k,j}} = \sum_{i=1}^{NC} \frac{\psi_{x,j} - \psi_{l,i,j}}{r_{l,i,j}} = \sum_{i=1}^{NC} L_{i,j} \frac{\rho_{vs,i,j} - \rho_{v,i}}{r_{s,i,j} + r_{h,i,j}} \quad [1]$$

Here,  $T_j$  is total transpiration rate ( $\text{kg m}^{-2} \text{ s}^{-1}$ ) for plant species  $j$  within the plant canopy;  $\psi_k$ ,  $\psi_{x,j}$ , and  $\psi_{l,i,j}$  are water potential ( $m$ ) in layer  $k$  of the soil, in the plant xylem and in the leaves of canopy layer  $i$ ;  $r_{r,k,j}$  and  $r_{l,i,j}$  are the resistance to water flow ( $\text{m}^3 \text{ s kg}^{-1}$ ) through the roots of layer  $k$  and the leaves of layer  $i$  for plant species  $j$ ;  $\rho_{vs,i,j}$  and  $\rho_{v,i}$  are the vapor density ( $\text{kg m}^{-3}$ ) within the stomatal cavities (assumed to be saturated vapor density) and of the air within the canopy layer;  $r_{s,i,j}$  and  $r_{h,i,j}$  are the stomatal resistance and leaf boundary layer resistance ( $\text{s m}^{-1}$ ) per unit of leaf area index ( $L_{i,j}$ ) within canopy layer  $i$  for plant species  $j$ ; and NS and NC are the number of soil and canopy layers.

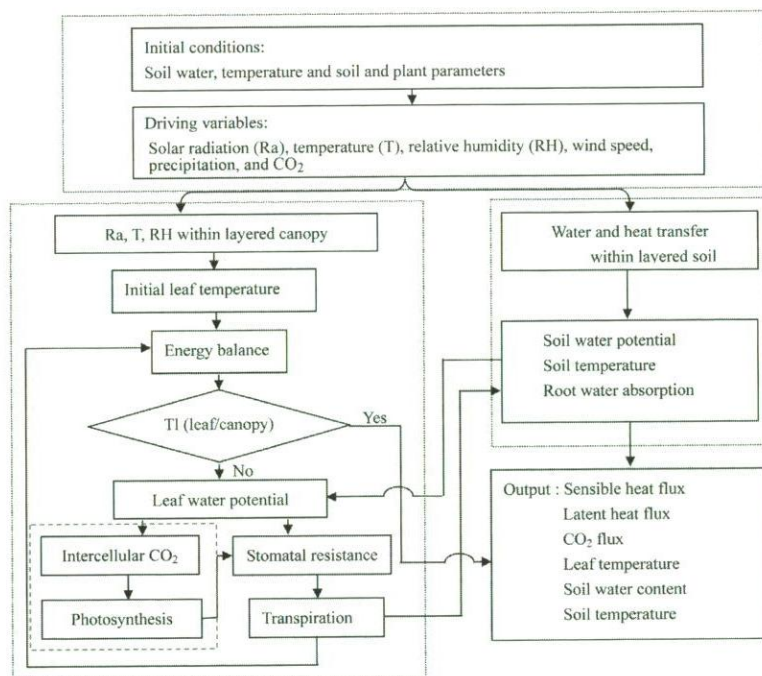


Fig. 7-1. Feedbacks and calculation scheme in the integrated SHAW and photosynthesis model (SHAW-Pn). The box isolated by dashed lines represents photosynthesis module.

SHAW adopted a simple equation relating stomatal resistance,  $r_s$ , to leaf water potential,  $\psi_l$  (Campbell, 1985), to simulate stomatal conductance:

$$r_s = r_{so} \left[ 1 + (\psi_l / \psi_c)^n \right] \quad [2]$$

where  $r_{so}$  is stomatal resistance with no water stress (assumed constant),  $\psi_c$  is a critical leaf water potential at which stomatal resistance is twice its minimum value, and  $n$  is an empirical coefficient.

Sensitivity of model simulations to stomatal resistance parameters was presented by Flerchinger and Pierson (1997);  $n$  has typically been set to 5 while  $\psi_c$  has been used for calibration and to reflect plant characteristics (Flerchinger et al., 1996a; Flerchinger and Pierson, 1997). Equations relating stomatal resistance to leaf temperature, vapor pressure deficit, soil moisture deficit, and solar irradiance have been developed (e.g., Dolman, 1993; Mihailovic and Ruml, 1996); however, estimation of a separate parameter is required for each of these factors. Because these factors all have an indirect effect on leaf water potential, the above relation is very effective in estimating stomatal resistance. However, incorporation of a photosynthesis model will allow the model to be more directly responsive to the



above factors. SHAW and this extended SHAW-Pn have no plant growth module. Therefore, plant height and leaf area index (LAI) are observational values and provided as inputs in the simulations.

### The Photosynthesis Model

The photosynthesis model can be divided into two parts: (i) the stomatal model, describing the relation of intercellular  $\text{CO}_2$  concentration ( $C_i$ ) with atmospheric  $\text{CO}_2$  concentration ( $C_s$ ), atmospheric vapor pressure deficit ( $D_a$ ) and leaf water potential ( $\psi_l$ ), i.e.,  $C_i = f(C_s, D_a, \psi_l)$ ; and (ii) the biochemical model describing the relation between  $C_i$  and photosynthetic rate ( $P_n$ ), light intensity ( $I$ ), and air temperature ( $T_a$ ), i.e.,  $P_n = f(I, T_a, C_i)$ .

#### Stomatal Models

Simulating stomatal response to environmental conditions can be quite complex. Timlin et al. (2008, this book) present an overview of approaches for simulating stomatal response. Tuzet and Perrier (2008, this book) simulated the effects of plant water storage capacity on stomatal conductance. Kremer et al. (2008, this book) computed stomatal conductances and transpiration separately for sunlit and shaded leaves. We chose here to express stomatal conductance ( $g_s$ ) as a semi-empirical function of humidity and ambient  $\text{CO}_2$  concentration ( $C_s$ ) over leaf surface, and photosynthetic rate ( $P_n$ ) (Ball et al., 1987; Leuning, 1995; Monteith, 1995; Wang and Leuning, 1998; Yu et al., 2004):

$$g_s = m \frac{P_n}{C_i - \Gamma} f(D_a / D_0) + g_0 \quad [3]$$

where  $\Gamma$  is the  $\text{CO}_2$  compensation point,  $D_0$  is a parameter with the same dimension as vapor pressure deficit ( $D_a$ ), and  $m$  and  $g_0$  are additional empirical parameters, which can include water conductance from epidermis. Introducing leaf water potential ( $\psi_l$ ) as a function of  $D_a/D_0$ ,  $g_s$  can be described as follows (Tuzet et al., 2003):

$$g_s = m \frac{P_n}{C_i - \bar{A}} f(\psi_l) + g_0 \quad [4]$$

The function  $f(\psi_l)$  is an empirical logistic equation describing the dependence of stomatal conductance to leaf water potential (Tuzet et al., 2003):

$$f(\psi_l) = \frac{1 + \exp(s_l \psi_f)}{1 + \exp[s_l(\psi_f - \psi_l)]} \quad [5]$$

where  $\psi_f$  is a reference leaf water potential and  $s_l$  is a sensitivity parameter. The stomatal conductance is depressed at moderate water deficits mostly because of decrease in leaf water potential (Chaves, 1991).

Stomatal resistance in the original SHAW (Eq. [2]) is responsive only to leaf water potential, whereas the stomatal conductance model above (Eq. [4]) demonstrates stomatal responses to changes in light, temperature,  $D_a$ ,  $\text{CO}_2$ , and soil water. Therefore, Eq. [4] was adopted in SHAW-Pn to replace Eq. [2].

### Biochemical Reaction of Photosynthesis

A biochemical model of photosynthesis for  $C_3$  plants was adopted according to Farquhar et al. (1980) and von Caemmerer and Farquhar (1981), in which photosynthetic rate was expressed as a function of intercellular  $\text{CO}_2$  concentration ( $C_i$ ), photosynthetic photon flux density ( $I$ ), and leaf temperature ( $T_l$ ). In this model, biochemical processes were described reflecting reactions in chloroplast excluding stomatal regulation, in which  $C_i$  was taken as an input variable (Collatz et al., 1991).

From gradient-flux relationship,

$$P_n = g_s(C_s - C_i) \quad [6]$$

Assuming  $g_0$  near 0, intercellular  $\text{CO}_2$  concentration ( $C_i$ ) can be obtained by combining Eq. [4] and Eq. [6] (Yu et al., 2002)

$$C_i = C_s - \frac{1}{m}(C_s - \Gamma)/f(\psi_l) \quad [7]$$

This equation gives a simple way to calculate  $C_i$  from atmospheric  $\text{CO}_2$  concentration ( $C_s$ ) and leaf water potential ( $\psi_l$ ).

Plant and soil respiration are components of  $\text{CO}_2$  flux from the system, and their rates can be represented as a  $Q_{10}$  function of temperature. Daytime soil respiration is relatively low compared with canopy photosynthesis. In the SHAW-Pn model, plant respiration was related to air temperature, and soil respiration was expressed as a function of soil temperature at 5 cm beneath the surface. The values of  $Q_{10}$  were adopted from Yu et al. (2007).

### Coupling of SHAW with the Photosynthesis Model

As with the original SHAW model, the plant canopy within SHAW-Pn was divided into layers with leaf area increments of  $0.5 \text{ m}^2 \text{ m}^{-2}$ . The SHAW model components provide leaf water potential for the stomatal model to calculate intercellular  $\text{CO}_2$  through stomatal control in each layer within the canopy, and also provide solar radiation to the biochemical model to calculate photosynthetic rate.  $\text{CO}_2$  concentration is assumed to be homogeneous within the canopy. Stomatal conductance was a function of  $P_n$  in Eq. [4], which replaced Eq. [2] in the original SHAW model and provided feedback in SHAW-Pn to calculate heat and water transfer in a leaf energy balance (Fig. 7-1).

Photosynthesis influences transpiration and energy balance through its correlation with stomatal conductance. The photosynthesis model was incorporated with SHAW through calculating stomatal conductance, which was used to solve leaf water potential and leaf temperature within the leaf energy balance (Fig. 7-1). Newton-Raphson iterations of the leaf energy balance are assumed to converge when the difference in leaf temperature for subsequent iterations is lower than a prescribed tolerance ( $0.01^{\circ}\text{C}$  in this study).

## Experimental Data

Field experiments were conducted to measure leaf gas exchange and mass and energy fluxes in a winter wheat cropping system. These data were used to validate the photosynthesis model and the performance of SHAW before and after coupling with the photosynthesis and stomatal models. The plant growth and soil water were also measured to provide state variables.

### Management and General Measurements

The experiment was conducted at Yucheng Comprehensive Experiment Station ( $36^{\circ}50' \text{ N}$ ,  $116^{\circ}34' \text{ E}$ , 28 m above sea level) of Chinese Academy of Sciences, North China Plain in 2003. The soil is silt loam. The site has a temperate monsoon climate with rainfall concentrated in summer and rarely occurring through the wheat growth period during winter and spring; water was supplemented by flood irrigation with ample N supply. Plants were oriented in north-south rows with recommended sowing density. Winter wheat variety was Zixuan 1. During the growing season, the LAI was measured every 5 d by harvesting 10 plants and measuring leaf area by LI-3100 (LI-COR Inc., Lincoln, NE) within a plot of  $1 \text{ m}^2$ , in which plants were counted.

### Leaf Gas Exchange Measurement

The infrared  $\text{CO}_2$  analysis system, LI-COR 6400 (LI-COR Inc.), was used to measure transpiration, photosynthetic rates, and stomatal conductance of the wheat leaves. The light and  $\text{CO}_2$  response curve of gas exchange, and stomatal conductance of flagged leaves were measured in the field from tillering stage to maturity (29 Mar.–June 2003). The instrument (LI-COR 6400) varied the light intensities from 0 to  $2000 \mu\text{mol m}^{-2} \text{ s}^{-1}$  for each measurement, while temperature, humidity, and wind speed over leaf were kept constant. Similarly,  $\text{CO}_2$  concentrations changed from 0 to  $1000 \mu\text{mol mol}^{-1}$  in the leaf chamber to get  $\text{CO}_2$  response separately. The system was calibrated and showed stable performance. Yu et al. (2002, 2004) used this same method for photosynthetic and stomatal response curve measurements.



## Flux Measurement

Fluxes of  $\text{CO}_2$  and latent and sensible heat over a wheat canopy were measured by eddy covariance method during the wheat growth period. A three-dimensional sonic anemometer (Model CSAT3, Campbell Scientific, Inc., Logan, UT) and an open path infrared gas analyzer (IRGA; Model LI-7500, LI-COR, Inc.) mounted at a height of 2.80 m measured the three components of the wind velocity vector, temperature and the densities of water vapor and  $\text{CO}_2$ . Soil heat flux was measured with a heat flux sensor (HFP01, Hukseflux, Netherlands) installed 0.05 m below soil surface. Data from the site had good energy balance closure during periods of weak advection (Lee and Yu, 2004; Yu et al., 2007) and were used for model comparison.

## Microclimate

Ambient weather conditions of temperature, relative humidity, wind direction, wind speed, and soil heat flux were measured with a temperature–humidity probe (HMP45C, Vaisala, Helsinki, Finland), a potentiometer windvane (Model W200P, Vector, UK), an anemometer (A100R, Vector, UK), and a barometer (CS105, Vaisala, Finland). The total and net radiation data were collected with a pyranometer (CM11, Kipp & Zonen, Canada) and a net four-component radiometer (CNR-1, Kipp & Zonen, Delft, Netherlands). The instruments above were located at a height of 2.80 m from the ground.

Soil temperatures were measured by an array of soil thermocouples (TCAV, Campbell Scientific, Logan, UT) installed in profiles at the depths of 0.00, 0.10, 0.20, and 0.50 m. Soil water content was measured by eight water content reflectometers (CS616\_L, Campbell Scientific, Logan, UT) at the depths of 0.00, 0.05, 0.10, 0.15, 0.20, 0.40, 0.60, and 1.0 m from soil surface.

## Model Tests and Validation

In this study, we first tested the dependence of simulated photosynthesis, transpiration and stomatal conductance on light and  $\text{CO}_2$  levels with field observations. We then analyzed the sensitivity of leaf water potential and related variables ( $C_i$ ,  $g_s$ ,  $T_r$  evapotranspiration and  $\text{CO}_2$  fluxes) to light intensity and diurnal weather variation. Finally, net radiation, water, sensible heat, and  $\text{CO}_2$  fluxes over the crop field were simulated by the coupled SHAW-Pn model.

Soil physical and plant physiological parameters used in the simulations were adapted from Yu et al. (2007). Plant physiological parameters (e.g., catalytic capacity of Rubisco, initial photon efficiency, critical leaf water potential, and initial leaf and root hydraulic resistances) are listed in Table 7–1, which

Table 7-1. Values of parameters used in the simulation.

Parameter	Value	Description and source
$\alpha_1$	212.0 kJ mol <sup>-1</sup>	Parameter in photosynthesis model (Collatz et al, 1991)
$\alpha_2$	703.0 kJ mol <sup>-1</sup> K <sup>-1</sup>	Parameter in photosynthesis model (Collatz et al, 1991)
$\psi_c$	-2 MPa	Critical leaf water potential used in stomatal resistance model
$C_0$	100.0 $\mu$ mol mol <sup>-1</sup> or 10 Pa	Michaelis-Menten constant in photosynthesis model
$D_0$	1500 Pa	Parameter in stomatal model, Eq. [2] and [3]
$\psi_f$	-1 MPa	Reference leaf water potential in stomatal model
$m$	8	Parameter in stomatal model, Eq. [2] and [3]
$r$	0.015	Ratio of respiration to maximum catalytic capacity of Rubisco in Eq.[11] (Collatz et al., 1991)
$R$	8.314 Jmol <sup>-1</sup> K <sup>-1</sup>	The universal gas constant (Collatz et al., 1991)
$R_0$	0.11 mg m <sup>-2</sup> s <sup>-1</sup>	Soil respiration rate at 25°C
$s_i$	0.05	Sensitivity parameter of $g_s$ to $\psi_f$
$r_i$	$1 \times 10^5$ m <sup>3</sup> s kg <sup>-2</sup>	Initial resistance of leaves (this study)
$r_r$	$2 \times 10^5$ m <sup>3</sup> s kg <sup>-2</sup>	Initial resistance of roots (this study)
$r_{s0}$	100.0 s m <sup>-1</sup>	Stomatal resistance with no water stress (this study)
$V_0$	55.0 $\mu$ mol m <sup>-2</sup> s <sup>-1</sup>	Catalytic capacity of Rubisco (Yu et al., 2002)
$\alpha_0$	0.06 $\mu$ mol m <sup>-2</sup> s <sup>-1</sup>	Initial photon efficiency (Yu et al. (2002) and 2004)
$\beta$	0.95	Convexity of light response curve (Yu et al., 2002, 2004)
$\Gamma$	50 $\mu$ mol mol <sup>-1</sup>	CO <sub>2</sub> compensation point (Yu et al. , 2002, 2004)
$\Gamma'$	5 Pa	Partial pressure of CO <sub>2</sub> at compensation point (this study)
$n$	5	Parameter in stomatal model, Eq. [1]

were obtained according to experimental data reflecting the physiological characteristics and leaf photosynthesis observations. Initial leaf and root hydraulic resistances and minimum stomatal resistance are from default values of the original SHAW model. The CO<sub>2</sub> flux is the sum of assimilation rate and plant and soil respiration rate over a unit ground area, of which the flux components are negative downward. The model was first parameterized against nighttime data when only the respiration component needed to be considered. The model was then used to simulate CO<sub>2</sub> flux before calibration against daytime measurements. A separate dataset during the growth period was used, and the parameters were kept unchanged throughout the vegetative growth, i.e., a portion of the data during the growth period was used for calibration and the rest for validation. In the model comparison, stomatal parameters for the original SHAW model (Eq. [2]) were from Xiao et al. (2006) and that for Eq. [4] used in SHAW-Pn were from Yu et al. (2007); parameter values for both equations are given in Table 7-1. The models

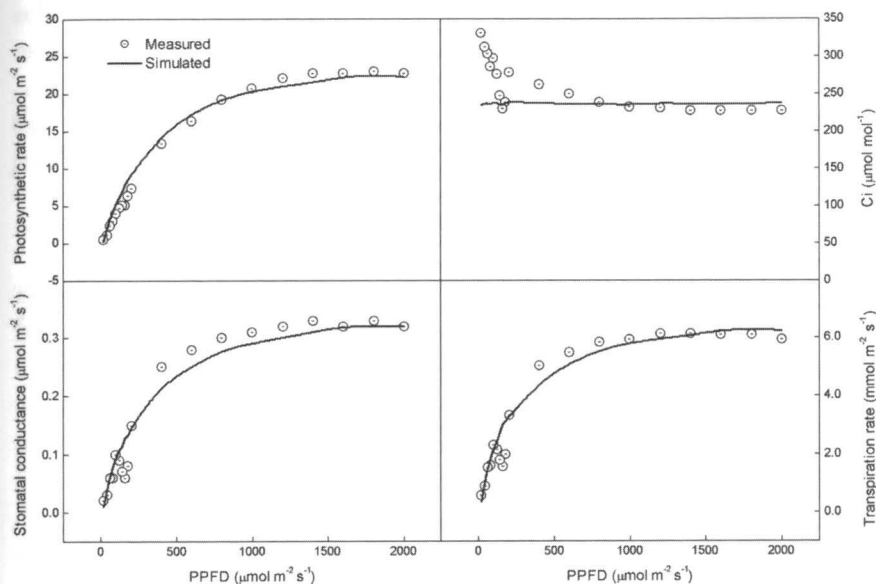


Fig. 7-2. Simulated and measured leaf photosynthesis, transpiration, intercellular  $\text{CO}_2$  concentration, and stomatal conductance in response to change in light intensities ( $I$ ).  $I$  ranged from 0 to 2000  $\mu\text{mol m}^{-2} \text{s}^{-1}$ , and parameters in the photosynthesis model were from Yu et al. (2002, 2004) (Yucheng, 20 Apr. 2003).

were driven by the meteorological variables to simulate fluxes of  $\text{CO}_2$  and latent and sensible heat.

### Responses of Photosynthesis, Transpiration, and Stomatal Conductance to Light Intensity and Carbon Dioxide Concentration

Physiological parameters were evaluated on the basis of data from intensive measurements collected on 20 Apr. 2003 for varying light intensities and on 24 April for varying  $\text{CO}_2$  concentration (Table 7-1). Both varying environments were set by the measurement system. The model was run to simulate responses of photosynthesis, transpiration, stomatal conductance, and  $\text{C}_i$  to light and  $\text{CO}_2$  concentration, while other factors were kept unchanged in the simulations. The  $\Gamma$  was obtained, and  $P_{\text{max}}$ ,  $m$ , and  $D_0$  were adjusted so that the relation between simulated and measured  $P_n$  achieved the highest correlation coefficient. A similar method was used by Yu et al. (2002, 2004).

Figure 7-2 illustrates comparisons of simulated and measured photosynthetic rate, transpiration rate, stomatal conductance, and  $\text{C}_i$  for varying light intensities. The light response curve for photosynthetic rate can be approximated with a Michaelis-Menten curve. Transpiration rate and stomatal conductance

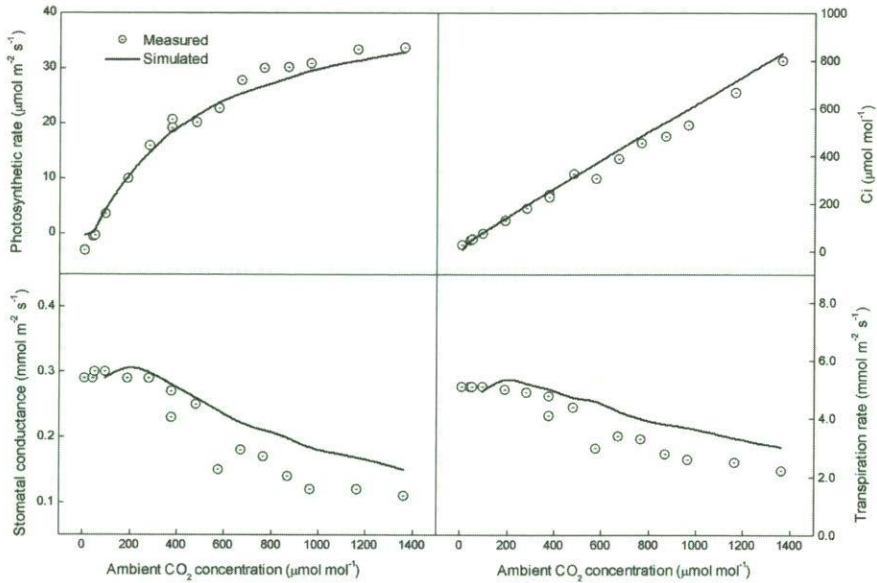


Fig. 7-3. Simulated and measured leaf photosynthesis, transpiration, intercellular  $\text{CO}_2$  concentration, and stomatal conductance in response to changes in  $\text{CO}_2$ . Ambient  $\text{CO}_2$  concentration ranged from 0 to  $1400 \mu\text{mol mol}^{-1}$  (Yucheng, 24 Apr. 2003).

have similar response to light. The simulated values correspond well with the measured ones with coefficients of determination ( $R^2$ ) over 0.96. An increase in irradiance can cause an increase in photosynthesis, leading to a decrease in  $C_i$ . This causes stomata to open to let in more  $\text{CO}_2$  and thus compensate for the decrease in  $C_i$  (Yu and Wang, 1998). Irradiance also alters leaf temperature, which influences photosynthetic rate, as well as stomatal opening by changing vapor pressure deficit between stomatal pores and ambient air.

As seen in Fig. 7-2, the model predicts a relatively constant  $C_i$  with increasing  $I$ . Observed  $C_i$  may decrease with increasing  $I$ , but the change is not great over a wide range of  $I$  and is evident only when irradiance is weak (Fig. 7-2). Wong et al. (1985) found that  $P_n$  and  $g_s$  change in the same proportion, so that  $C_i$  changes very little over a wide range of  $I$ . In most of the species examined, when light intensity increases, photosynthesis and conductance increase, but  $C_i$  obviously decreases at low  $I$  and comes to a fairly constant value when light intensities are above 10% of full sunlight (Morison and Jarvis, 1983).

Figure 7-3 illustrates comparisons of simulated and measured photosynthetic rate, transpiration rate, stomatal conductance, and  $C_i$  for varying  $\text{CO}_2$  concentrations. Increase in  $\text{CO}_2$  concentration will induce elevation in intercellular  $\text{CO}_2$  and an increase in photosynthetic rate (Fig. 7-3). However, stomatal



conductance decreases with increasing  $\text{CO}_2$ , thereby reducing transpiration. The model simulations accord well with these measurements. It shows that the intercept is near zero, so  $C_i/C_s$  is almost constant, as was found by many researchers, e.g., Wong et al. (1979, 1985), Sharkey and Raschke (1981), and Morison and Jarvis (1983) among others.

### Sensitivity of Photosynthesis, Transpiration, and Stomatal Conductance to Diurnal Weather Variation

The performance of SHAW-Pn was demonstrated by sensitivity of water and  $\text{CO}_2$  fluxes to diurnal change in environmental variables (solar radiation,  $\text{CO}_2$ , and temperature). The diurnal variations of solar radiation, air temperature, and relative humidity drive the change in leaf water potential when soil water is kept constant. Solar radiation flux density peaked at noon with maximum of  $855 \text{ W m}^{-2}$ , and air temperature reached its maximum of  $28^\circ\text{C}$  around 1400 h. Other atmospheric input variables were assumed constant during the day, i.e., wind speed was  $1.5 \text{ m s}^{-1}$  and ambient  $\text{CO}_2$  concentration  $350 \mu\text{mol mol}^{-1}$ . The assumed values of these variables are typical in midlatitude summers (Yu et al., 2001). Initial leaf water potential at 0600 h near sunrise was set equal to the average soil water potential over the rooting depth ( $-2 \text{ MPa}$ ). Simulated leaf water potential in response to diurnal variations of environmental factors is presented in Fig. 7-4. Leaf water potential started to decrease after sunrise, decreased sharply with the increase in solar radiation around noon, and remained near constant for much of the afternoon. It recovered from its lowest value under water-stressed condition during high atmospheric demand to reach the value of soil potential during the night. High solar radiation sustained high leaf temperatures and induced high water vapor deficit between stomatal cavity and ambient air, which may cause high transpiration and water loss, inducing stomatal closure as a feedback. Therefore, leaf water potentials in the upper canopy layers are lower than that in the

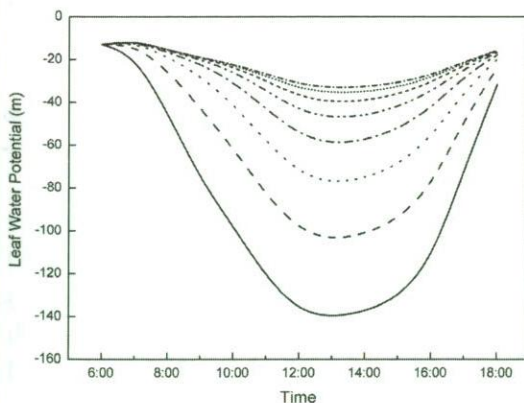


Fig. 7-4. Diurnal change in leaf water potential in response to varying solar radiation and temperature. Lines represent leaf potential of layers within canopy with leaf area increments of  $0.5 \text{ m}^2$  with the bottommost line representing the layer being nearest to the top of the canopy.

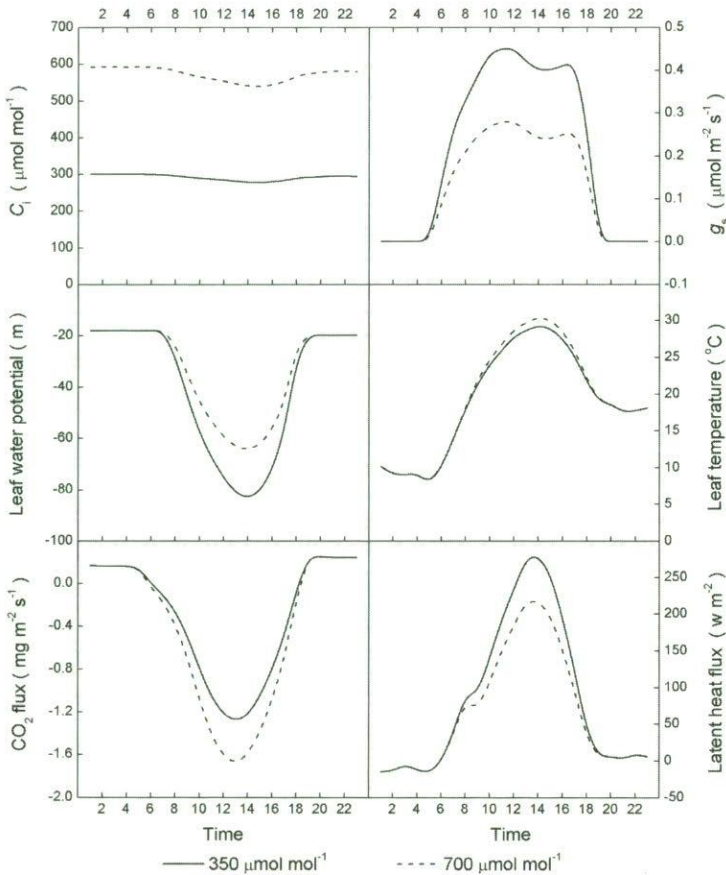


Fig. 7-5. Sensitivity analysis of diurnal changes in intercellular CO<sub>2</sub>, stomatal conductance, leaf water potential, leaf temperature, and CO<sub>2</sub> and water vapor fluxes under present CO<sub>2</sub> (350 μmol mol<sup>-1</sup>) and doubled CO<sub>2</sub> (700 μmol mol<sup>-1</sup>) concentrations.

lower layers. The simulated model sensitivity also demonstrated that maximum leaf temperature occurred in the afternoon causing the highest  $D_a$ , assuming constant water vapor pressure in air. Lowest leaf water potential roughly corresponded to the maximum temperature while solar radiation was still high, indicating that leaf water potential is greatly influenced by atmospheric evaporative demand under the relatively moist simulated soil water conditions.

The diurnal variations of  $C_i$ ,  $g_s$ , leaf water potential, leaf temperature, and CO<sub>2</sub> and water vapor fluxes were simulated under two scenarios of present (350 μmol mol<sup>-1</sup>) and doubled (700 μmol mol<sup>-1</sup>) ambient CO<sub>2</sub> concentrations (Fig. 7-5). The driving variables are the same as that in Fig. 7-4.  $C_i$  almost doubled with doubling of atmospheric CO<sub>2</sub>, which would decrease stomatal conductance and

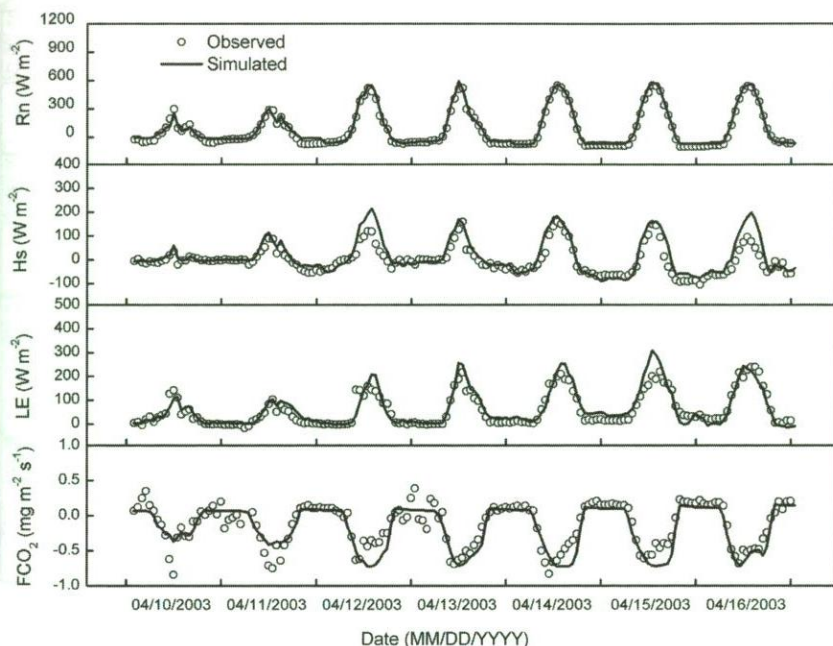


Fig. 7-6. Simulated net radiation, latent and sensible heat and  $\text{CO}_2$  fluxes over wheat canopy in the booting stage. (LAI = 2.3, Yucheng, 10–16 Apr. 2003).

promote photosynthetic rate. Accordingly, transpiration rate decreased and leaf water potential increased with decreased stomatal conductance. Thus, leaf temperature slightly increased when latent heat was restrained under doubled  $\text{CO}_2$  scenario. Although stomatal conductance slightly decreased in the afternoon (1400 h) because of high temperature and  $D_a$ , a dip in photosynthesis and transpiration is not noticeable because the higher solar radiation and temperature in the afternoon may increase  $P_n$  (Fig. 7-5). This compensates for the effects of stomatal closure on photosynthesis and transpiration.

### Simulation of Energy and Carbon Dioxide Fluxes over Wheat Canopy

The components of energy balance were simulated on several continuous days in the booting, heading, flowering, and milking stages from March to May when measured LAI ranged from 2.3 to 4.5.

Figure 7-6 shows hourly measured and simulated components of energy balance over seven continuous days in the booting stage during 10 to 16 April when LAI was 2.3. Solar radiation and temperature are relatively low during this period in the growing season. Net radiation reached  $600 \text{ W m}^{-2}$  at maximum around noon and sensible and latent heat fluxes were  $120$  and  $200 \text{ W m}^{-2}$  around



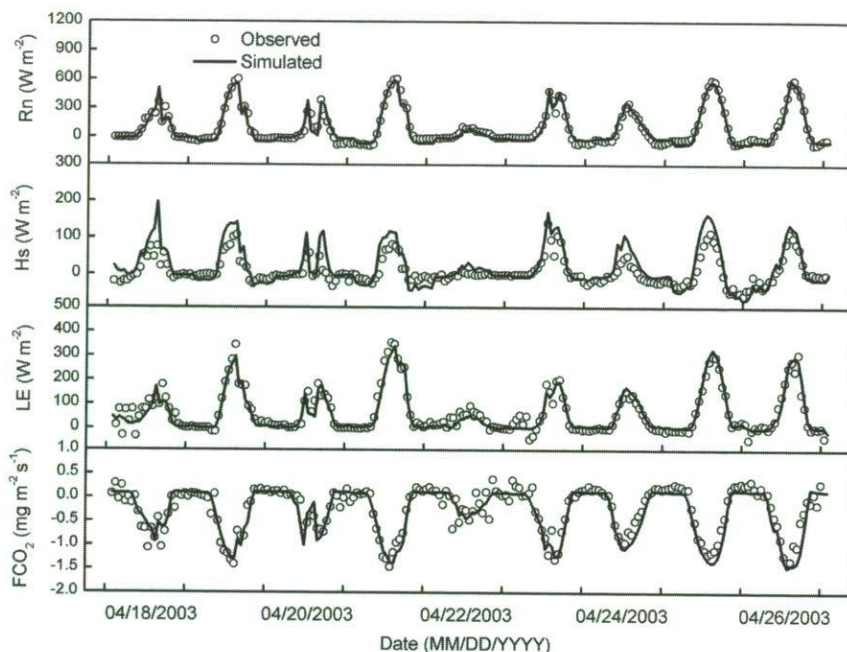


Fig. 7-7. Simulated net radiation, latent and sensible heat and CO<sub>2</sub> fluxes over wheat canopy in heading stage. (LAI = 3.0, Yucheng, 18–26 Apr. 2003).

noon, respectively. CO<sub>2</sub> flux reached the lowest value of  $-0.7 \text{ mg m}^{-2} \text{ s}^{-1}$ . Simulated values of net radiation corresponded closely with the measured values, and the general trends of simulated and observed CO<sub>2</sub> fluxes corresponded well. Figure 7-7 illustrates flux simulation in heading growth stage during 18 to 26 April with measured LAI of 3.0. There were some cloudy days when net radiation and sensible and latent heat fluxes were low. On clear days, CO<sub>2</sub> flux reached  $-1.2 \text{ mg m}^{-2} \text{ s}^{-1}$ , which was higher than the previous stage because of increase in solar radiation and air temperature. The model tracked the field measurements reasonably well, and the general trend of the simulation during the different periods is very similar to each other.

Figure 7-8 is an example of model performance during the bearing stage (27 April – 5 May) when measured LAI was 4.0. The trend of simulated water vapor flux agreed well with observed. The maximum net radiation exceeded  $650 \text{ W m}^{-2}$ , and the maximum latent heat flux was  $450 \text{ W m}^{-2}$ . The maximum sensible heat flux was only  $100 \text{ W m}^{-2}$ , which was lower than that in early growth stage. CO<sub>2</sub> flux peaked at about  $-1.3 \text{ mg m}^{-2} \text{ s}^{-1}$ . Simulated values of net radiation corresponded closely with the measured values, the general trends of simulated and



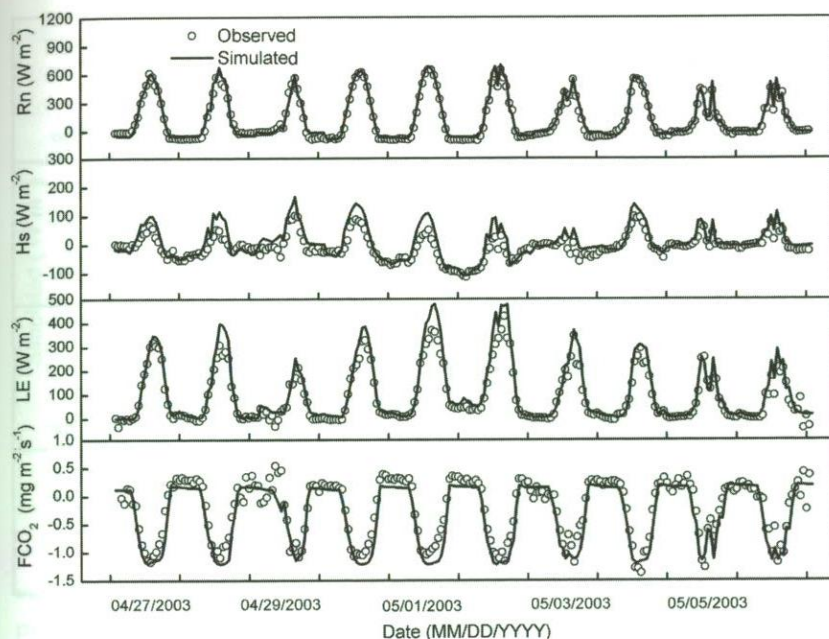


Fig. 7-8. Simulated net radiation, latent and sensible heat and  $CO_2$  fluxes over wheat canopy in bearing stage. (LAI = 4.0, Yucheng, 27 Apr.–6 May 2003).

observed  $CO_2$  fluxes corresponded well, and the general trend of the simulation during the different periods was very similar to each other.

Because of senescence in the milking stage, the plant canopy consisted of green transpiring leaves and nontranspiring yellow leaves. For simulation, the plant canopy was divided into two types: one with green leaf area capable of photosynthesis and transpiration and the other consisting of shriveled leaves and stems which intercepted solar radiation but did not assimilate and transpire. The green leaf area index (GLAI) was estimated to be 2.0 and 1.0 for shriveled leaf area index during this growth period according to harvested leaf biomass. The measured heights of green plants and shriveled plants were 0.9 and 0.7 m, respectively. During crop senescence (17–23 May), maximum net radiation was 600  $W m^{-2}$ , which was relatively low because of high crop albedo (Fig. 7-9). Latent heat still reached 300  $W m^{-2}$ .  $CO_2$  flux was simulated quite well with a minimum value of  $-1.0 mg m^{-2} s^{-1}$ . However, daytime  $CO_2$  and water vapor fluxes were overestimated if the effect of shriveled plants was not considered.

To sum up the simulation during the four growth stages, the prediction of net radiation and latent and sensible heat fluxes were fairly close to observed values with RMSEs (root-mean square error) of 36.1, 31.0, and 25.8  $W m^{-2}$ , respec-

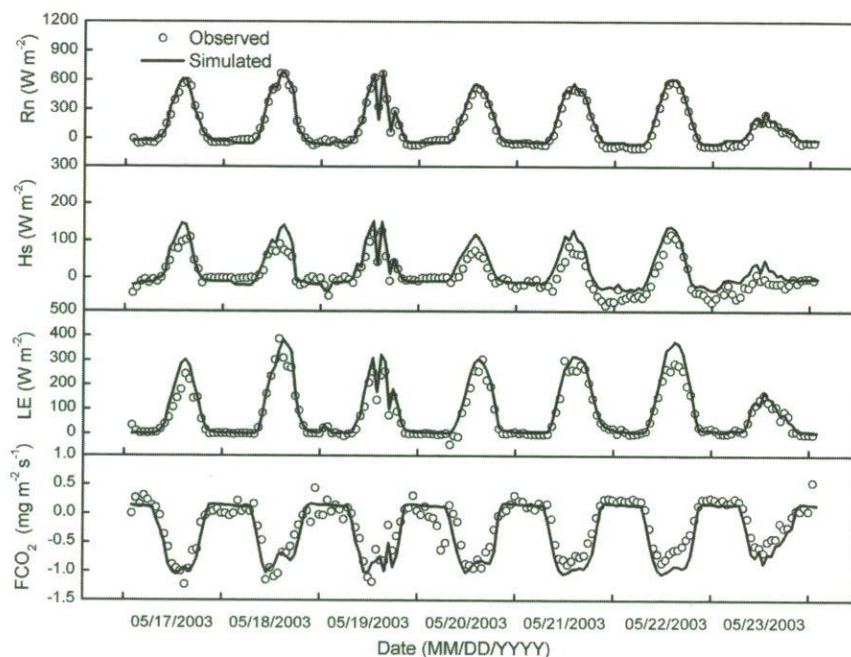


Fig. 7–9. Simulated net radiation, latent and sensible heat and  $\text{CO}_2$  fluxes over wheat canopy in milking stage. (GLAI = 2.0 and shriveled LAI = 1.0, Yucheng, 17–23 May 2003).

tively. The RMSE of  $\text{CO}_2$  flux ( $\text{FCO}_2$ ) simulation for all growth stages was  $0.18 \text{ mg m}^{-2} \text{ s}^{-1}$ . Hourly simulated and measured latent heat fluxes for the entire simulated period are presented in Fig. 7–10 for both SHAW and SHAW-Pn models.

## Discussion and Conclusions

Stomata play a key role in regulating the flow of water from the soil through the plants to the atmosphere. Stomatal conductance is known to respond to leaf temperature, vapor pressure deficit, soil moisture,  $\text{CO}_2$ , and solar irradiance (e.g., Dolman, 1993; Mihailovic and Ruml, 1996); however, estimation of a separate value for each of these interrelated influences is difficult. Because these factors all have an indirect effect on leaf water potential and stomatal opening (Jarvis, 1976), the SHAW model adopted a simple yet effective equation relating stomatal response to leaf water potential (Campbell, 1985). The effect of meteorological and soil variables on leaf water potential is expressed within SHAW through simulation of water flux through the soil–plant–atmosphere continuum. Similar work on simulating water and heat transfer in a canopy by considering non-steady-state leaf water potential was reported by Chen and Coughenour (1994) and Lhomme et al. (2001), among others. The SHAW model using the stomatal

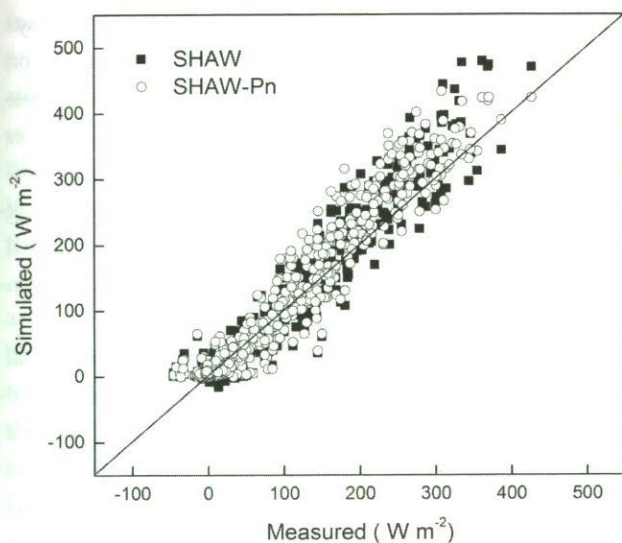


Fig. 7–10. Measured and simulated latent heat fluxes using the stomatal models (Eq. [1] and [4]) against measured values (Yucheng, 10Apr.–23 May 2003).

equation in Eq. [2] relating stomatal resistance to leaf water potential may comprehensively reflect the influence of solar radiation, temperature, humidity, and soil water and can also perform excellently in simulation of heat and water fluxes (Xiao et al., 2006).

The original SHAW model, however, cannot simulate  $\text{CO}_2$  flux and the influence of atmospheric  $\text{CO}_2$  on stomatal response. Linkage between SHAW and a photosynthesis model makes it more responsive to environmental influences on transpiration in addition to extending its function to simulate  $\text{CO}_2$  flux. SHAW-Pn computes stomatal conductance from photosynthetic rate and  $\text{CO}_2$  concentration. This makes stomatal conductance respond appropriately to changing  $\text{CO}_2$ . But, when we compared simulation from the two stomatal models (Eq. [2] and [4]), no significant difference was found in the surface energy fluxes between SHAW and SHAW-Pn (Fig. 7–10,  $r^2 = 0.93$  and  $0.94$  respectively). This means that the original SHAW model using the simple stomatal conductance model (Eq. [2]) can simulate water and heat fluxes well in field conditions with no significant change in atmospheric  $\text{CO}_2$ . Through sensitivity analysis, we demonstrated the ability of the stomatal model in SHAW-Pn to simulate the responses of photosynthesis and transpiration to changing  $\text{CO}_2$ , which the original SHAW cannot do.

Leaf water potential is a function of both atmospheric evaporative demand and soil water availability. Hence, several models have used Eq. [3] multiplied by a soil water function, rather than Eq. [4] (e.g., Wang and Leuning, 1998). The application of leaf water potential in Eq. [4] is a way to indirectly capture the influence of solar radiation, temperature, humidity, and soil water on stomatal response, which neither vapor pressure deficit nor a soil water function can do.



It was found that SHAW-Pn may tend to overestimate  $\text{CO}_2$  flux on some days (e.g., Fig. 7–8). This may be attributed to several potential factors. One limitation is that many nonstomatal responses are not included in the model. For example, photoinhibition may happen under high light intensity, temperature, or water stress, causing a decrease in photosynthetic rate (Yu et al., 2001). Additionally, we neglected the effect of leaf boundary layer on  $\text{CO}_2$  gas diffusion, which can be significant when wind speed is low. This boundary layer resistance can be included in the leaf scale model, but will increase the calculation in the coupled photosynthesis–transpiration–stomatal conductance model (Yu et al., 2001).

Many physical and physiological processes interact to control stomatal response. It is one of the basic tasks of physiological ecology to develop a comprehensive model and parameterize the processes. There are a series of interactions among biophysical, biochemical, and physiological processes when a plant is exposed to a change in environmental factors. Because solar radiation is the driving force for both photosynthesis and leaf energy balances, it influences physiological processes through photosynthesis and leaf temperature. Leaf temperature affects photosynthesis in two ways: the first is on the intrinsic speed of biochemical processes of photosynthesis, the other is on  $D_a$  through its effect on the intercellular saturated vapor pressure.  $C_i/C_s$  is determined mainly by the changes in  $g_s$  caused by changes in  $D_a$ , so the increase in temperature causes a decrease in  $C_i$ . Photosynthetic rate decreases with increasing  $D_a$ , because of stomatal closure. Around noon on clear days, solar radiation always exceeds the light saturation point, and therefore its increase does not noticeably promote photosynthesis. If air temperature reaches or exceeds its optimal value, the increase in solar radiation and the corresponding increases in leaf temperature and  $D_a$  will lead to a decrease in photosynthesis. Sensitivity analysis demonstrated that the photosynthesis model can be responsive to low leaf water potentials when soil water is low and atmospheric evaporation demand is high, which may bring about midday depression of photosynthesis and transpiration because of stomatal closure (Yu et al., 2002, 2007). SHAW-Pn did simulate a midday decrease in stomatal conductance but not sufficient under the simulated conditions to cause a noticeable change in photosynthesis or transpiration. A midday depression in transpiration may alleviate leaf water loss (Long et al., 1994; Hirasawa and Hsiao, 1999). These physiological responses may define the diurnal patterns of  $\text{CO}_2$  and water fluxes.

Under natural conditions, the magnitude of contribution of changes in each environmental factor to variations in assimilation may vary widely, and some factors and processes are dominant under a particular circumstance and may have little effect under others (Leverenz, 1994). For example, solar radiation changes



from zero to more than photosynthetic saturation point in a day. When water and temperature stresses are not serious, diurnal variation of photosynthesis is dominated by solar radiation. Therefore, the physiological model of photosynthesis uses light response curve as the core of the model, whereas the other factors exert their influence by affecting the values of some parameters in the model (Thornley, 1976). Parameterization of  $C_i$ , Eq. [5], is a key resolution of biochemical photosynthesis model, which is based on some observational data and stomatal models.

The photosynthesis model based on biochemical processes is widely used, at levels from leaf, canopy, and up to global scales (e.g., Hatton et al., 1992; Wirtz, 2000; Yu et al., 2001). There are some small differences in the mathematical description of parameters among such kinds of models. The SHAW-Pn model integrated the biochemical reaction of photosynthesis with a stomatal conductance model. It includes the influence of light, temperature, and relative humidity on photosynthesis and in turn on stomatal control and transpiration.

As SHAW does not include a component of crop growth and needs input of LAI, we simulate fluxes by giving leaf area index in each growth stage. Previous efforts have incorporated SHAW with Root Zone Water Quality Model (RZWQM), i.e., the RZ-SHAW model (Flerchinger et al., 2000). This SHAW-Pn does not consider simulation of crop growth to avoid error of LAI calculation. However, it can be incorporated into RZ-SHAW or other models such as RZWQM, which do have crop growth routines. This coupling will expand those models to include a biochemical model of photosynthesis. The soil respiration model is simple in SHAW-Pn, and it could be improved by linking it with a detailed nutrient cycling model such as in RZWQM. Coupling of transpiration and stomata conductance to plant-water potential similar to the scheme of SHAW-Pn has been reported previously (e.g., Bohrer et al., 2005; Chuang et al., 2006). However, SHAW is good at radiation exchange within canopy and energy balance for mixed canopies with multiple plant species and up to 10 canopy layers, while a big-leaf scheme was adopted in some other models (Tuzet et al., 2003). SHAW-Pn, therefore, could be incorporated into hydrological or regional-atmospheric models to provide a multilayer canopy energy balance as an alternative to the big-leaf approach.

Although the stomatal and photosynthesis model in SHAW-Pn can respond to changes in  $CO_2$ , temperature, and solar radiation, the photosynthetic capability and stomatal density of plants may acclimate over time to long-term  $CO_2$  increase (Woodward and Bazzaz, 1988). This change can be integrated into the short-term model response by adjusting model parameters. For example,  $m$  in Eq. [4] can compensate for changes in carboxylation activity of photosystem and sensitivity of stomatal conductance to environment as plants adjust over time in response

to CO<sub>2</sub> increase. Therefore, SHAW-Pn provides a tool to evaluate response of ecological processes in response to climate change.

## References

- Arora, V.K. 2003. Simulating energy and carbon fluxes over winter wheat using coupled land surface and terrestrial ecosystem models. *Agric. For. Meteorol.* 118:21–47.
- Ball, J.T., I.E. Woodrow, and J.A. Berry. 1987. A model predicting stomatal conductance and its contribution to the control of photosynthesis under different environmental conditions. p. 221–224. *In* I. Biggins (ed.) *Progress in photosynthesis research*. Martinus Nijhoff Publishers, the Netherlands.
- Bohrer, G., H. Mourad, T.A. Laursen, D. Drewry, R. Avissar, D. Poggi, R. Oren, and G.G. Katul. 2005. Finite element tree crown hydrodynamics model FETCH using porous media flow within branching elements: A new representation of tree hydrodynamics. *Water Resour. Res.* 41:W11404 10.1029/2005WR004181.
- Calvet, J.C. 2000. Investigating soil and atmospheric plant water stress using physiological and micrometeorological data. *Agric. For. Meteorol.* 103:229–247.
- Campbell, G.S. 1985. Transport models for soil-plant systems. p. 45–66. Elsevier, Amsterdam, the Netherlands.
- Chaves, M.M. 1991. Effects of water deficits on carbon assimilation. *J. Exp. Bot.* 42:1–16.
- Chen, D.X., and M.B. Coughenour. 1994. GEMTM: A general model for energy and mass transfer of land surfaces and its application at the FIFE sites. *Agric. For. Meteorol.* 68:145–171.
- Choudhury, B.J., and J.L. Monteith. 1988. A four-layer model for heat budget of homogeneous land surfaces. *Q. J. R. Meteorol. Soc.* 114:373–398.
- Chuang, Y.L., R. Oren, A.L. Bertozzi, N. Phillips, and G.G. Katul. 2006. The porous media model for the hydraulic system of a conifer tree: From sap flux data to transpiration rate. *Ecol. Modell.* 191:447–468.
- Collatz, G.J., J.T. Ball, C. Grivet, and J.A. Berry. 1991. Physiological and environmental regulation of stomatal conductance, photosynthesis and transpiration: A model that includes a laminar boundary layer. *Agric. For. Meteorol.* 54:107–136.
- Cowan, I.R. 1965. Transport of water in the soil-plant-atmosphere system. *J. Appl. Ecol.* 2:221–239.
- Dolman, A.J. 1993. A multiple source land surface energy balance model for use in general circulation models. *Agric. For. Meteorol.* 65:21–45.
- Farquhar, G.D., S. von Caemmerer, and J.A. Berry. 1980. A biochemical model of photosynthetic CO<sub>2</sub> assimilation in leaves of C<sub>3</sub> species. *Planta* 149:78–90.
- Flerchinger, G.N. 2000. The Simultaneous Heat and Water SHAW Model: Technical Documentation. Technical Report NWRC-2000–09, USDA-ARS, Northwest Watershed Research Center, Boise, Idaho, Electronic Document: <http://www.nwrc.ars.usda.gov/models/SHAW/downloads.html>; verified 23 May 2008.
- Flerchinger, G.N., R.M. Aiken, K.W. Rojas, and L.R. Ahuja. 2000. Development of the root zone water quality model RZWQM for over-winter conditions. *Trans. ASAE* 43:59–68.
- Flerchinger, G.N., J.M. Baker, and E.J.A. Spaans. 1996a. A test of the radiative energy balance of the SHAW model for snowcover. *Hydrol. Process.* 10:1359–1367.
- Flerchinger, G.N., K.R. Cooley, and Y. Deng. 1994. Impacts of spatially and temporally varying snowmelt on subsurface flow in a mountainous watershed: 1. Snowmelt simulation. *Hydrol. Sci. J.* 39:507–520.
- Flerchinger, G.N., and C.L. Hanson. 1989. Modeling soil freezing and thawing on a rangeland watershed. *Trans. ASAE* 32:1551–1554.
- Flerchinger, G.N., C.L. Hanson, and J.R. Wight. 1996b. Modeling of evapotranspiration and surface energy budgets across a watershed. *Water Resour. Res.* 32:2539–2548.
- Flerchinger, G.N., W.P. Kustas, and M.A. Weltz. 1998. Simulating surface energy fluxes and radiometric surface temperatures for two arid vegetation communities using the SHAW model. *J. Appl. Meteorol.* 37:449–460.



- Flerchinger, G.N., and F.B. Pierson. 1991. Modeling plant canopy effects on variability of soil temperature and water. *Agric. For. Meteorol.* 56:227–246.
- Flerchinger, G.N., and F.B. Pierson. 1997. Modeling plant canopy effects on variability of soil temperature and water: Model calibration and validation. *J. Arid Environ.* 35:641–653.
- Flerchinger, G.N., and K.E. Saxton. 1989. Simultaneous heat and water model of a freezing snow-residue-soil system: I. Theory and development. *Trans. ASAE* 32:573–578.
- Flerchinger, G.N., T.J. Sauer, and R.A. Aiken. 2003. Effects of crop residue cover and architecture on heat and water transfer at the soil surface. *Geoderma* 116:217–233.
- Hatton, T.J., J. Walker, W.R. Dawes, and F.X. Dunin. 1992. Simulations of hydroecological responses to elevated CO<sub>2</sub> at the catchment scale. *Aust. J. Bot.* 40:679–696.
- Hirasawa, T., and T.C. Hsiao. 1999. Some characteristics of reduced leaf photosynthesis at midday in maize growing in the field. *Field Crop Res.* 62:53–62.
- Jarvis, P.G. 1976. The interpretation of the variations in water potential and stomatal conductance found in canopies in the field. *Philosophical Trans. Royal Soc. B-Biol. Sci. (Ser. B)* 273:593–610.
- Jarvis, P.J., and K.G. McNaughton. 1986. Stomatal control of transpiration: Scaling up from leaf to region. In *Advances in Ecological Research*, Vol. 15. Academic Press, London.
- Kremer, C., C.O. Stöckle, A.R. Kemanian, and T. Howell. 2008. A canopy transpiration and photosynthesis model for evaluating simple crop productivity models. p. 165–190. In L. Ahuja et al. (ed.) *Response of crops to limited water: Understanding and modeling water stress effects on plant growth processes*. *Advances in Agricultural Systems Modeling Ser. 1*. ASA, CSSA, SSSA, Madison, WI.
- Lakshmi, V., and E.F. Wood. 1998. Diurnal cycles of evaporation using a two-layer hydrological model. *J. Hydrol.* 204:37–51.
- Lee, X.H., and Q. Yu. 2004. Micrometeorological fluxes under the influence of regional and local advection: A revisit. *Agric. For. Meteorol.* 122:111–124.
- Leuning, R. 1995. A critical appraisal of a combined stomatal-photosynthesis model for C<sub>3</sub> plants. *Plant Cell Environ.* 18:339–355.
- Leuning, R., F.M. Kelliher, D.G.G. De Pury, and E.D. Schulze. 1995. Leaf nitrogen, photosynthesis, conductance and transpiration: Scaling from leaves to canopies. *Plant Cell Environ.* 18:1183–1200.
- Leverenz, J.W. 1994. Factors determining the nature of the light dosage response curve of leaves. p. 239–254. In N.R. Baker and J.R. Bowyer (ed.) *Photoinhibition of photosynthesis from molecular mechanisms to the field*. BIOS Scientific Publishers, Oxford, UK.
- Lhomme, J.P., A. Rocheteau, J.M. Ourcival, and S. Rambal. 2001. Non-steady-state modelling of water transfer in a Mediterranean evergreen canopy. *Agric. For. Meteorol.* 108:67–83.
- Long, S.P., S. Humphries, and P.G. Falkowski. 1994. Photoinhibition of photosynthesis in nature. *Annu. Rev. Plant Biol.* 45:633–662.
- McMurtrie, R.E., R. Leuning, W.A. Thompson, and A.M. Wheeler. 1992. A model of canopy photosynthesis and water use incorporating a mechanistic formulation of leaf CO<sub>2</sub> exchange. *For. Ecol. Manage.* 52:261–278.
- Mihailovic, D.T., and M. Ruml. 1996. Design of land-air parameterization scheme LAPS for modeling boundary layer surface processes. *Meteorol. Atmos. Phys.* 58:65–81.
- Monteith, J.L. 1995. A reinterpretation of stomatal responses to humidity. *Plant Cell Environ.* 18:357–364.
- Morison, J.I.L., and P.G. Jarvis. 1983. Direct and indirect effects of light on stomata. II. In *Commelina communis*. *Plant Cell Environ.* 6:103–109.
- Sharkey, T.D., and K. Raschke. 1981. Separation and measurement of direct and indirect effects of light on stomata. *Plant Physiol.* 68:33–40.
- Thornley, J.H.M. 1976. *Mathematical models in plant physiology*. p. 86–110. Academic Press, London.
- Timlin, D., J. Bunce, D. Fleisher, V.R. Reddy, Y. Yang, S.-H. Kim, S.A. Saseendran, and B. Quebedeaux, and. 2008. Simulation of the effects of limited water on photosynthesis and transpiration in field crops: Can we advance our modeling approaches? p. 105–144. In L. Ahuja et al. (ed.) *Response of crops to limited water: Understanding and modeling water stress effects on*

- plant growth processes. *Advances in Agricultural Systems Modeling Ser. 1*. ASA, CSSA, SSSA, Madison, WI.
- Tuzet, A., and A. Perrier. 2008. Modeling the dynamics of water flow through plants, role of capacitance in stomatal conductance, and plant water relations. p. 145–164. *In* L. Ahuja et al. (ed.) *Response of crops to limited water: Understanding and modeling water stress effects on plant growth processes*. *Advances in Agricultural Systems Modeling Ser. 1*. ASA, CSSA, SSSA, Madison, WI.
- Tuzet, A., A. Perrier, and R. Leuning. 2003. A coupled model of stomatal conductance, photosynthesis and transpiration. *Plant Cell Environ.* 26:1097–1116.
- von Caemmerer, S., and G.D. Farquhar. 1981. Some relationships between the biochemistry of photosynthesis and the gas exchange of leaves. *Planta* 153:376–387.
- Wang, Y.P., and R. Leuning. 1998. A two-leaf model for canopy conductance, photosynthesis and partitioning of available energy I: Model description and comparison with a multi-layered model. *Agric. For. Meteorol.* 91:89–111.
- Williams, M., E.B. Rastetter, D.N. Fernandes, M.L. Goulden, S.C. Wofsy, G.R. Shaver, J.M. Melillo, J.W. Munger, S.M. Fan, and K.J. Nadelhoffer. 1996. Modelling the soil-plant-atmosphere continuum in a Quercus-Acer stand at Harvard Forest: The regulation of stomatal conductance by light, nitrogen and soil/plant hydraulic properties. *Plant Cell Environ.* 19:911–927.
- Wirtz, K.W. 2000. Second order up-scaling: Theory and an exercise with a complex photosynthesis model. *Ecol. Modell.* 126:59–71.
- Woodward, F.I., and F.A. Bazzaz. 1988. The response of stomatal density to CO<sub>2</sub> partial pressure. *J. Exp. Bot.* 39:1771–1781.
- Wong, S.C., I.R. Cowan, and G.D. Farquhar. 1979. Stomatal conductance correlates with photosynthetic capacity. *Nature* 282:424–426.
- Wong, S.C., I.R. Cowan, and G.D. Farquhar. 1985. Leaf conductance in relation to rate of CO<sub>2</sub> assimilation. I. influence of nitrogen nutrition, phosphorus nutrition, photon flux density, and ambient partial pressure of CO<sub>2</sub> during ontogeny. *Plant Physiol.* 78:821–825.
- Xiao, W., Q. Yu, G.N. Flerchinger, and Y.F. Zheng. 2006. Evaluation of SHAW model in simulating energy balance, leaf temperature and micrometeorological variables within a maize canopy. *Agron. J.* 98:722–729.
- Yu, Q., J. Goudriaan, and T.D. Wang. 2001. Modeling diurnal courses of photosynthesis and transpiration of leaves on the basis of stomatal and non-stomatal responses, including photoinhibition. *Photosynthetica* 39:43–51.
- Yu, Q., Y.F. Liu, J.D. Liu, and T.D. Wang. 2002. Simulation of leaf photosynthesis of winter wheat on Tibetan Plateau and in North China Plain. *Ecol. Modell.* 155:205–216.
- Yu, Q., and T.D. Wang. 1998. Simulation of the physiological responses of C<sub>3</sub> plant leaves to environmental factors by a model which combines stomatal conductance, photosynthesis and transpiration. *Acta Bot. Sin.* 40:551–566.
- Yu, Q., S.H. Xu, J. Wang, and X.H. Lee. 2007. Influence of leaf water potential on diurnal changes in CO<sub>2</sub> and water vapour fluxes. *Bound-Lay Meteorol.* 124:161–181.
- Yu, Q., Y.Q. Zhang, Y.F. Liu, and P.L. Shi. 2004. Simulation of the stomatal conductance of winter wheat in response to light, temperature and CO<sub>2</sub> changes. *Ann. Bot. (London)* 93:435–441.